BMC Cancer

RESEARCH

Open Access

Decitabine-mediated DNA methylation dynamics at pericentromeric satellite 2 repeats

Enrica Sordini[1], Eugenia Ciurlia[1], Alessia Zanella[1], Benedetta Fogliardi[1], Dorela Lame[2], Antonella Poloni[2], Stefano Amatori[1*†] and Mirco Fanelli[1*†]

Abstract

The hypomethylating agents (HMAs) 5-azacytidine (vidaza-AZA) and 5-aza-2′-deoxycytidine (decitabine-DAC) are part of the standard of care for the treatment of myelodysplastic syndromes (MDS) and acute myeloid leukemia (AML). However, the molecular events mediated by HMAs in MDS and AML are poorly understood, and the efficacy of MDS and AML treatments is still improvable. The majority of CpG dinucleotides are located at satellite repeats, and their methylation levels are known to play a fundamental role in ensuring the genomic stability of cells. HMAs are believed to act through a plethora of effects, including DNA demethylation and the consequent re-expression of aberrantly silenced genes, DNA damage due to the covalent trapping of DNA methyltransferases (DNMTs) on DNA, and endogenous retroelements (EREs) reactivation associated with the induction of a cell-intrinsic antiviral response. DNA demethylation of satellite repeats and the consequent genomic destabilization and mitotic impairment of leukemic cells are also believed to play important roles. Although the demethylating activity of HMAs on gene promoters has been extensively investigated, little is known about their effects on satellite DNA methylation during treatment, especially when the selective pressure of the treatment ends. Here, we characterized the dynamics of satellite 2 DNA methylation mediated by decitabine in a human AML cell line model (U937 cells). We demonstrate that the initial demethylation of satellite 2 repeats is followed by complete recovery after 48 h of culture. The observed regain of methylation is associated with increased expression of DNMT3B, the de novo DNMT known to target satellite 2 repeats. In the intent of deciphering the regulation of DNMT3B expression, we found that DAC significantly increased the level of H3 acetylation at the DNMT3B promoter. These preliminary data shed light on DAC-mediated methylation dynamics at satellite 2 repeats, suggesting that satellite 2 remethylation could limit the genomic-destabilizing effects mediated by HMAs in tumor cells and, thus, the future evaluation of strategies to impair this methylation regain and to improve HMAs activity against tumor cells.

†Stefano Amatori and Mirco Fanelli contributed equally to this work.

*Correspondence:
Stefano Amatori
stefano.amatori@uniurb.it
Mirco Fanelli
mirco.fanelli@uniurb.it

Full list of author information is available at the end of the article

Keywords Hypomethylating agents, DNA demethylating agents, Decitabine, DNA methylation, Satellite 2, DNA methyltransferases, Acute myeloid leukemia

Introduction

Approximately 20 years after their initial approval, the hypomethylating agents (HMAs) 5-azacytidine (vidaza—AZA) and 5-aza-2′-deoxycytidine (decitabine—DAC), also known as azanucleosides, remain the mainstays of treatment for high-risk myelodysplastic syndromes (MDS) and acute myeloid leukemia [1, 2], two heterogeneous groups of clonal hematopoietic disorders that share several common molecular alterations (e.g., mutations of specific genes and activation of inflammatory signaling pathways) [3, 4].

HMAs are incorporated into DNA during replication and function to covalently trap DNA methyltransferase enzymes (DNMTs), leading to the global loss of DNA methylation. By reactivating aberrantly silenced genes, HMA-mediated hypomethylation potentially affects DNA repair, cell cycle control, apoptosis, cell signaling, angiogenesis and the control of cancer cell invasion and metastasis [5, 6]. In addition, other mechanisms have been proposed, such as the activation of a DNA damage response due to the trapping of DNMTs on DNA [7] and the reactivation of endogenous retroelements (EREs) and the consequent induction of a cell-intrinsic antiviral response [8].

Unfortunately, the median overall survival of patients subjected to HMA monotherapy is approximately 13–16 months for patients with MDS [9] and less than one year for AML patients [10], indicating the need for improved therapies.

In the human genome, CpGs are abundant in centromeric and pericentromeric satellite DNA and within repeat elements in noncoding intergenic areas [11]. Interestingly, CpGs in repetitive elements are more efficiently demethylated by azanucleosides than are gene-associated CpGs, suggesting that these elements are important targets of HMA demethylating activity [12].

It has been suggested that the demethylation of satellite sequences might promote chromosome instability and tumorigenesis [13, 14]. However, owing to the relatively high replication rate and consequent HMAs genomic incorporation in cancer cells, acute demethylation of satellite DNA induced by HMAs could contribute to their therapeutic effect, especially in models such as MDS and AML, in which repeat elements demethylation, which is frequently found in other types of cancer, is an extremely rare event [15]. Several observations indeed demonstrate that azanucleoside-induced demethylation of pericentromeric repetitive sequences is associated with high chromosome instability and consequent mitotic defects in normal and tumor cell models. For example, AZA and DAC were found to induce chromosome missegregation, deletions, chromosome breaks and condensation of pericentromeric regions on chromosomes 1, 9, and 16 [16]. Similarly, pericentromeric regions demethylation mediated by decitabine was found to be associated with aneuploidy and mitotic defects in HCT-116 cells [17]. In addition, chromosomal segregation errors in chromosomes 1 and 16 have been associated with satellite 2 demethylation in azacytidine-treated human lymphocytes [18].

DAC is normally administered at a dosage of 20 mg/m^2 per day for five days of treatment every 28 days. Owing to its very short half-life in human plasma, DAC is administered daily in one-hour intravenous infusions. This means that, normally, approximately one hour of exposure to DAC is followed by several hours of drug-free resting and that 5 days of treatment are followed by 23 days of intervals during each cycle [19]. Although the demethylating effects of azanucleosides have been widely investigated, little is known about the effects of azanucleosides on repetitive satellite DNA methylation levels, especially when the selective pressure of the treatment ends (between daily treatments of each cycle and between cycles).

Here, we investigated the dynamics of the effects of HMAs on satellite 2 methylation in the human AML U937 cell line and, concomitantly, the associated changes in the expression and epigenetic features of the genes involved in DNA methylation in response to azanucleoside treatment.

Materials and methods

Cell culture, treatments and cell survival evaluation

The U937 cell line was maintained in RPMI 1640 medium supplemented with 10% fetal bovine serum (FBS, Gibco, Paisley, UK), 1% L-glutamine (Lonza, Verviers, Belgium) and 1% penicillin/streptomycin (Euroclone, Pero, MI, Italy) in a humidified atmosphere at 37 °C with 5% CO_2. The cell lines were originally obtained from the ATCC repository and were routinely tested via PCR and MycoAlert (Lonza, Verviers, Belgium #LT07-318) for mycoplasma contamination by the European Institute of Oncology (Milan, Italy).

Decitabine (Sigma, Saint Louis, MO, USA) and vidaza (Sigma, Saint Louis, MO, USA) treatments were performed at the reported doses and timings. At the end of the treatments, the cells were counted via a CellDrop automatic cell counter (DeNovix, Wilmington, DE, USA), and the percentage of survival was calculated with respect to the untreated cellular population.

Satellite 2 and DNMT3B promoter methylation analysis

Pericentromeric satellite 2 CpG methylation levels were monitored via Southern blotting analysis as described previously [20] via a satellite 2 probe obtained via PCR in the presence of DIG-11-dUTP as a tracer (Roche, Mannheim, Germany) via primer pairs that are able to amplify a 400 bp region of satellite DNA: sat2–384U (5′-A TGGAAATGAAAGGGGTCATCATCT-3′) and sat2–781L (5′-ATTCGAGTCCATTCGATGATTCCA T-3′) [21].

Methylation-sensitive high-resolution melting (MS-HRM) analysis of DNMT3B promoter was performed as previously described [22]. Genomic DNA was purified via the DNeasy Blood and Tissue Kit following the manufacturer's instructions (Qiagen, Hilden, Germany). DNA was quantified with a Qubit 2.0 fluorimeter (Thermo Fisher Scientific, Waltham, USA) and bisulfite modified with the Epitect Bisulfite Kit (Qiagen, Hilden, Germany) according to the manufacturer's protocol. Bisulfite-converted DNA was used as template for PCR amplification and subsequent HRM analysis. The standards included in the EpiTect PCR Control DNA Set (Qiagen, Hilden, Germany), which represents fully methylated and fully unmethylated DNA, were also amplified.

PCR amplification and HRM analysis were conducted via a Rotor-Gene 6000 (Corbett Research, Sydney, Australia) instrument. The primers used were designed with Methyl Primer Express software (Thermo Fisher Scientific, Waltham, USA) to amplify a 327 bp product containing 24 CpG sites in the center of the DNMT3B CpG island (from + 406 to + 732 with respect to the TSS). The sequences of primers used were as follows: 3B-MetF: 5'-GGGAGAGATTTTTTTTAGGGA-3' and 3B-MetR: 5'-AACCAAATAATTACACCCCCT-3'. PCR amplification was carried out in a final volume of 25 µl containing FastStart SYBR Green Master Mix (Roche, Mannheim, Germany), 360 nM of each primer and 2 ng of bisulfite-treated DNA template. The thermal profile was 10 min at 95 °C followed by 40 cycles of 30 s at 95 °C, 30 s at 59 °C, and 30 s at 72 °C. HRM was performed by ramping from 69 °C to 85 °C and increasing by 0.1 °C every 2 s.

Real-time RT–qPCR

Total RNA was extracted from treated or untreated U937 cells via an RNeasy Mini Kit (Qiagen, Hilden, Germany) and reverse transcribed into cDNA via SuperScript IV Reverse Transcriptase (Thermo Fisher Scientific, Vilnius, Lithuania) following the manufacturer's instructions.

The cDNA was then amplified via FastStart SYBR Green Master Mix (Roche, Mannheim, Germany) and primer pairs as previously described [21].

Real-time qPCR assays and subsequent data collection were performed with a Rotor-Gene 6000 robocycler (Corbett Research, Sydney, Australia). The expression levels of the target genes were normalized to that of glyceraldehyde 3-phosphate dehydrogenase (GAPDH), and the relative quantification analysis was based on the 2-ΔΔCt method [23].

Chromatin immunoprecipitation (ChIP)

After being washed in PBS, the cells were resuspended in fixation buffer (5 mM HEPES pH 7.5, 10 mM NaCl, 0.1 mM Na2EDTA, 0.05 mM EGTA, and 1% formaldehyde) and fixed for 10 min at 37 °C. After centrifugation, the samples were resuspended in 0.5 mL of lysis buffer (10 mM Tris–HCl pH 7.4, 0.15 M NaCl, 3 mM $CaCl_2$, 2 mM $MgCl_2$, 0.5% Tween 20, 1 mM PMSF and 10 µg/mL RNase A—Roche, Mannheim, Germany) and incubated for 30 min at room temperature on a rotating platform. Unless otherwise specified, all the centrifugations were performed at 17,860 × g for 3 min at + 4 °C. After resuspension in 0.3 mL of extraction buffer (10 mM Tris–HCl pH 7.4, 0.15 M NaCl, 3 mM $CaCl_2$, 2 mM $MgCl_2$, 0.1% SDS), the samples were sonicated with three pulses of 30 s each, interrupted by 60 s pulses, in a thermoblock refrigerated at − 20 °C, with an amplitude of 40% using an EpiShear sonicator (Active Motif, Carlsbad, CA, USA). After being cleared by centrifugation (9500 × g for 5 min at room temperature), the supernatants containing chromatin were saved, and an aliquot of 30 µL was purified via the PCR Purification Kit (Qiagen, Hilden, Germany) and used for DNA amount estimation by Qubit (Invitrogen, Eugene, OR, USA) using the dsDNA HS Assay Kit (Invitrogen, Eugene, OR, USA) and to control the chromatin size via agarose gel electrophoresis. Chromatin immunoselection was conducted as previously described [24] using anti-H3K4me3 (#39,159, Lot. 01609004; Active Motif, Carlsbad, CA, USA), anti-H3K27me3 (#07–449, Lot. JBC1873477; Millipore, Temecula, CA, USA), anti-H3K9 (#39,161, Lot. 13,509,002; Active Motif, Carlsbad, CA, USA) or anti-acetylated H3 (#06–599, Lot. DAM1513997; Millipore, Temecula, CA, USA) antibodies. The extracted DNA, once purified and quantified by Qubit 2.0 fluorimeter (Thermo Fisher Scientific, Waltham, USA), was analyzed by real-time q-PCR using the following primer pairs: VCL-F: 5'-ATGCCAG TGTTTCATACGCG-3', VCL-R: 5'-CGCCCTCCTCG TGCATTAT-3', COL2A1-F: 5-CTTTCGAGGCTGGC GAACT-3', COL2A1-R: 5'-CGGTTCAGGTTACAGC CCA-3', DNMT1-F: 5-CTCTCTCCGTTTGGTACAT CCC-3', DNMT1-R: 5'-CTTTTCGCGCGGAAACC-3', DNMT3A-F: 5'-TCAAGGCAGCTCATCTCAGAGA-3', DNMT3A-R: 5-CAGCCAGGTGCCGCC-3', DNMT3B-F: 5'-GGGTGAGGAAACGTCCACG-3', DNMT3B-R: 5'-CAGCCAGGTGCCGCC-3', sat2–384U: 5′-A TGGAAA TGAAAGGGGTCATCATCT-3′, sat2–781L: 5′-ATTCG AGTCCATTCGATGATTCCAT-3′.

Results

Azanucleoside-induced satellite 2 demethylation is followed by rapid remethylation at satellite 2 repeats

Similar to what happens in vivo, the stability of azanucleosides in aqueous solutions at 37 °C is extremely short. The estimated DAC half-life ranges from 4–10 h, whereas AZA is even less stable, with a reported half-life of only 1.5 h [25–30]. This means that the dose of drug administered at the beginning of the in vitro treatments decreases rapidly and that the main effect of the drugs is exerted during the first hours of treatment. Thus, time points of 16 and 64 h were chosen to monitor "early" and "late" effects, allowing the cells to be essentially free of drug during the last hours of the experiment, as happens in patients between daily administrations and between treatment cycles [19]. These dose–response experiments were also performed to identify the best conditions for subsequent experiments.

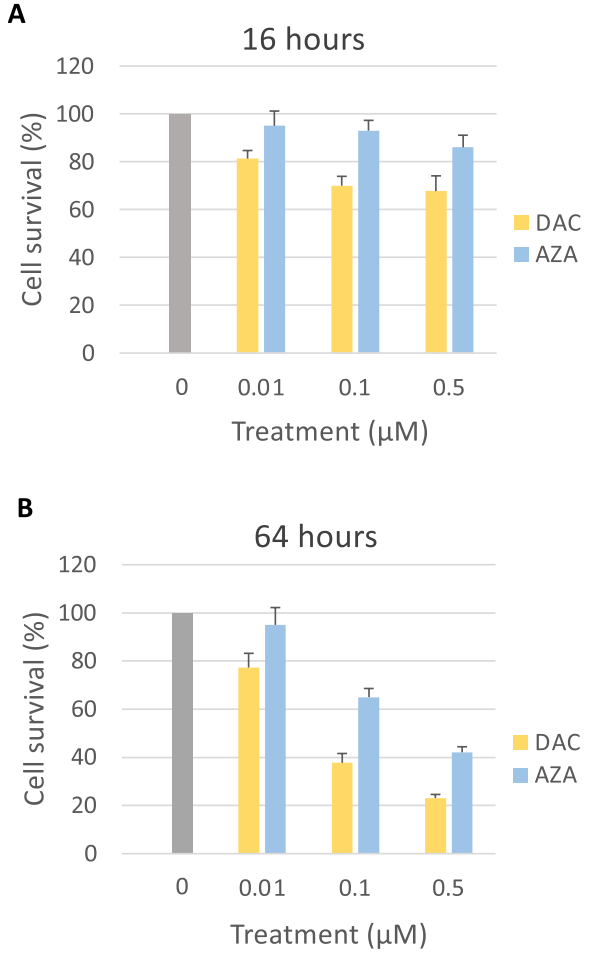

Fig. 1 Effects of decitabine (DAC) and azacytidine (AZA) on the survival of U937 cells. Dose–response experiments were conducted at 16 h (**A**) and 64 h (**B**) of treatment. U937 cells were subjected to treatments at the reported concentrations or left untreated, and at the end of the treatments, the cells were counted via the Trypan blue dye exclusion technique through an automatic cell counter. All the experiments were conducted in triplicate

As expected, both AZA and DAC resulted in a time- and dose-dependent reduction in cell survival, with DAC showing greater efficacy than AZA (Fig. 1).

On the basis of the cell survival results, the concentrations of 0.01 and 0.1 μM, which are in line with the plasma concentration of the drug normally found in DAC-treated patients [31, 32], were chosen for subsequent experiments in consequence of the lower impact on cell viability monitored at 64 h of exposure respect to the higher dose of 0.5 μM, avoiding the risk of analyze samples that have been subjected to extreme treatment conditions. For the same reason, longer times of exposure were not considered in this study.

The effects of DAC on the methylation levels of satellite 2 repeats were investigated via a methylation-sensitive restriction enzyme assay followed by Southern blotting against satellite 2 repeats. A DAC-induced reduction in satellite 2 methylation was detected at a concentration of 0.1 μM and, to a lesser extent, at 0.01 μM after 16 h of treatment. However, after further 48 h of culture, U937 cells regained satellite 2 methylation at both concentrations tested (Fig. 2). AZA treatments at concentrations of 0.1 μM and 0.5 μM caused a reduction in cell survival comparable to that induced by DAC at 0.01 μM and 0.1 μM resulted in similar results, corroborating this observation (Additional Fig. 1, panel A).

Azanucleoside treatments increase DNMT3B expression

The possible modulation of DNA methyltransferase expression levels was investigated as a function of DAC-induced satellite 2 demethylation. The relative abundances of the maintenance methyltransferase DNMT1 and the de novo methyltransferases DNMT3A and DNMT3B were investigated by real-time quantitative PCR (qPCR). The active DNMT3B isoforms, DNMT3B1 and DNMT3B2, were studied together via a common primer pair that is able to amplify both transcripts (DNMT3B1/2), and inactive DNMT3B3 was also investigated because of its known regulatory role [33, 34]. As shown in Fig. 3, significant upregulation of both the DNMT3B1/2 and DNMT3B3 isoforms was detected after 16 h (1.96- and 1.47-fold, respectively) of DAC treatment at a final concentration of 0.1 μM, which further increased after 64 h (2.46- and 1.82-fold, respectively), whereas no fluctuations were observed in the expression levels of the other DNMTs.

Similar upregulation of DNMT3B isoforms was observed when U937 cells were treated with 0.5 μM AZA for 64 h (Additional Fig. 1, panel B).

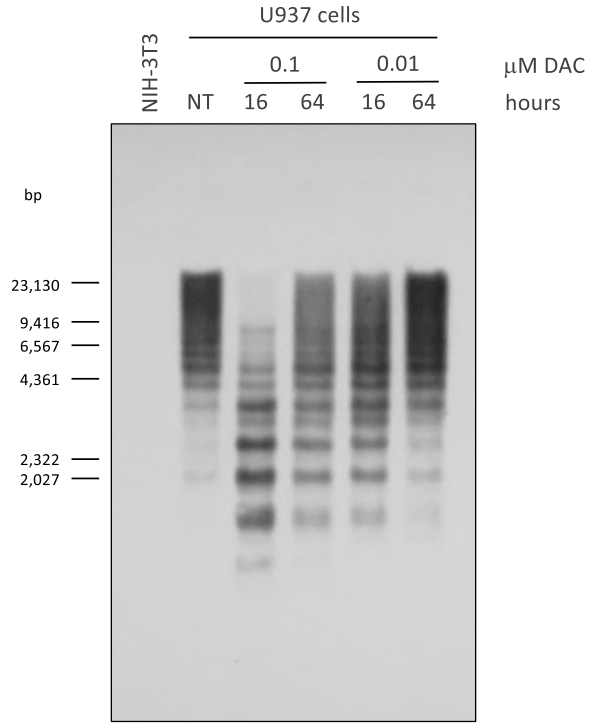

Fig. 2 Effects of decitabine on the methylation status of satellite 2 repeats in U937 cells. U937 cells were subjected to treatments with DAC at the reported concentrations and times or left untreated (NT). At the end of the treatments, genomic DNA was purified and digested via the Csp45I enzyme, separated via 1% agarose gel electrophoresis, blotted, and hybridized by a satellite 2 PCR probe (sat2-384U/781L). Ethidium bromide-stained agarose gel prior of DNA transfer is shown in Additional Fig. 3, while full-length blot is reported in Additional Fig. 5 (panels **A**, **B**). NIH-3T3: murine fibroblast cell line used as negative control of satellite 2 probe binding

Effects of azanucleosides on DNA methylation and histone PTMs at the DNMT3B promoter

We subsequently evaluated whether the monitored DNMT3B upregulation was associated with changes in the methylation levels of its promoter. The methylation status of the DNMT3B promoter CpG island was analyzed via a methylation-sensitive high-resolution melting (MS-HRM) assay in U937 cells exposed to decitabine at concentrations of 0.01 and 0.1 μM for 16 and 64 h. First, we found that the DNMT3B promoter was scarcely methylated in U937 cells (Fig. 4). When treated with DAC, U937 cells showed a slight decrease in methylation, which was clearly distinguishable only after 64 h of treatment at a concentration of 0.1 μM (Fig. 4). Even in this case, treatment with 0.5 μM AZA produced similar results (Additional Fig. 1, panel C).

DNA methylation and histone PTMs are highly interconnected and influence each other. To clarify the mechanism responsible for the observed DNMT3B upregulation, we focused on histone PTMs. For this purpose, three histone PTMs, encompassing the most studied types of histone H3 methylation, were investigated via chromatin immunoprecipitation (ChIP) in U937 cells treated with DAC at a concentration of 0.1 μM for 64 h. Attention has been given to H3K4me3, normally found at active gene promoters, the gene silencing-associated PTM H3K27me3, and H3K9me3, the heterochromatin marker representing the histone H3 PTM most closely related to DNA methylation [35]. Moreover, histone H3 acetylation has also been investigated because of its plasticity and known interplay with DNA methylation [36–38]. In addition to the DNMT1, DNMT3A and DNMT3B promoters, vinculin (VCL) and collagen type II alpha 1 chain (COL2A1) enrichments were also evaluated in the untreated samples as controls for active and silent gene enrichment, respectively. As expected, VCL and COL2A1 enrichment demonstrated the specificity of the four immunoprecipitations, since the first was enriched in histone PTMs normally associated with active transcription (H3K4me3 and H3ac), whereas the latter was enriched in gene silencing-associated histone PTMs (H3K27me3 and H3K9me3; Fig. 5). With respect to DNMTs, we observed

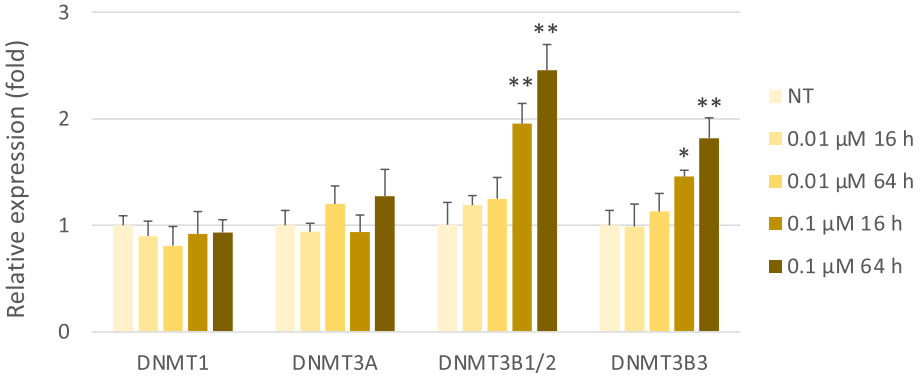

Fig. 3 Effects of DAC on the expression of DNMTs. U937 cells were subjected to treatments with DAC at the reported concentrations and times or left untreated. At the end of the treatments, total RNA was purified, reverse transcribed into cDNA and amplified by real-time qPCR using primer pairs specific for the transcripts of different DNMTs (GAPDH was also amplified and used for normalization). Relative quantitation was performed via the 2^{-ddCt} method. All the experiments were conducted in triplicate. *$P < 0.05$ with respect to the untreated sample (NT); **$P < 0.01$ with respect to the NT sample

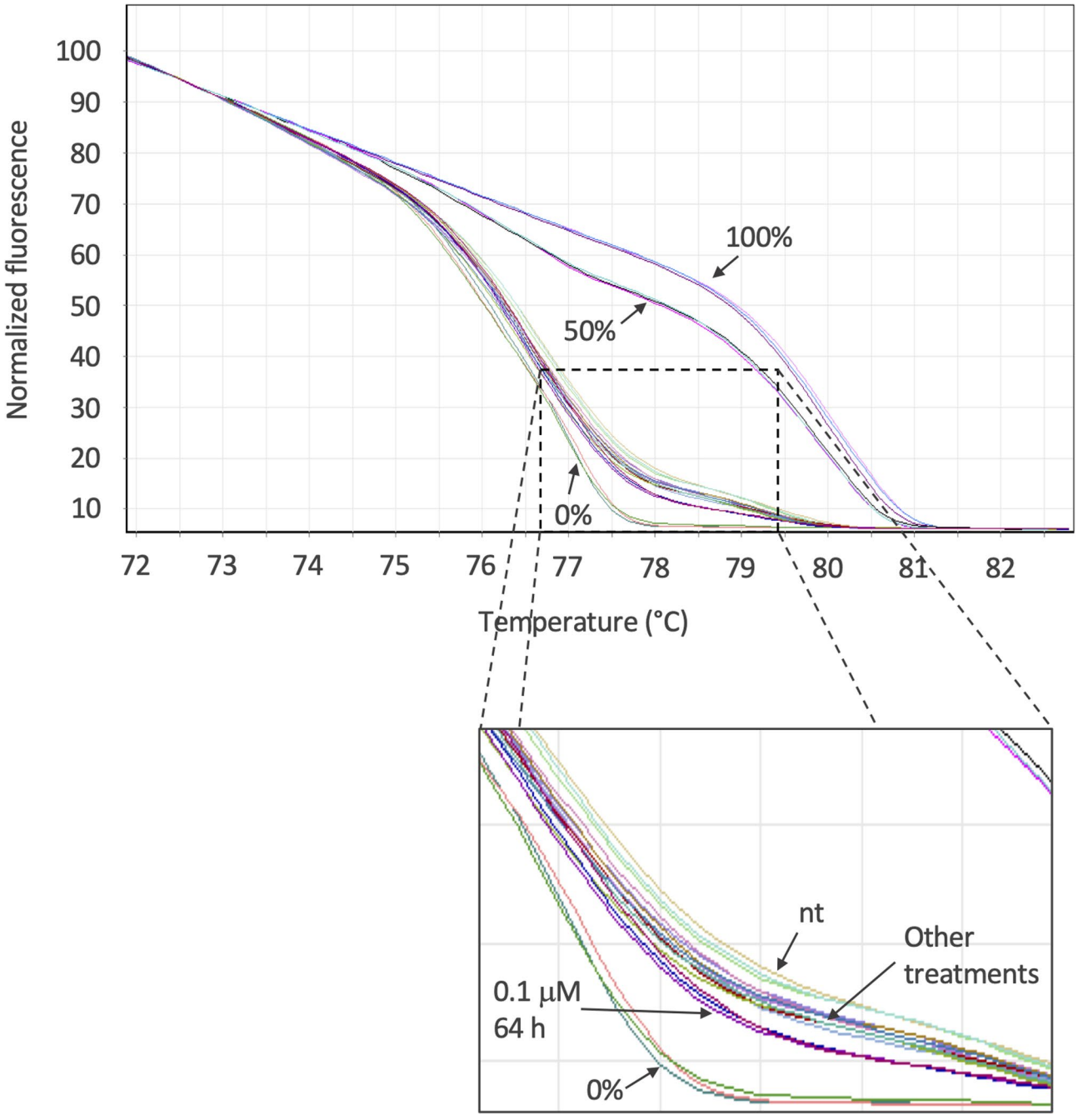

Fig. 4 Effects of DAC on DNMT3B promoter methylation. The methylation status of the DNMT3B promoter was investigated via methylation-sensitive high-resolution melting (MS-HRM). U937 cells were subjected to treatments with DAC at the reported concentrations and times or left untreated. At the end of the treatments, the genomic DNA was purified, subjected to bisulfite conversion and amplified by PCR using primers specific for the DNMT3B promoter. The resulting PCR products were analyzed by HRM, and the fluorescence signal was normalized using the Rotor-Gene Q software. 100%, 0% and 50% are commercial DNA standards representing fully methylated, fully unmethylated and a 1:1 mix of fully methylated and fully unmethylated DNA, respectively. All the experiments were conducted in triplicate

lower levels of silencing-associated histone PTMs at the DNMT1 promoter than de novo DNMTs did. However, no significant changes were detected in the levels of the three types of histone methylation at DNMT promoters after DAC treatment. In contrast, a significant increase in H3 acetylation was observed at the DNMT3B promoter (Fig. 5).

Satellite 2 repeats were also investigated showing, as expected, high levels of H3K9me3 and H3K27me3 and low levels of H3K4me3 and H3ac. Interestingly, a slight

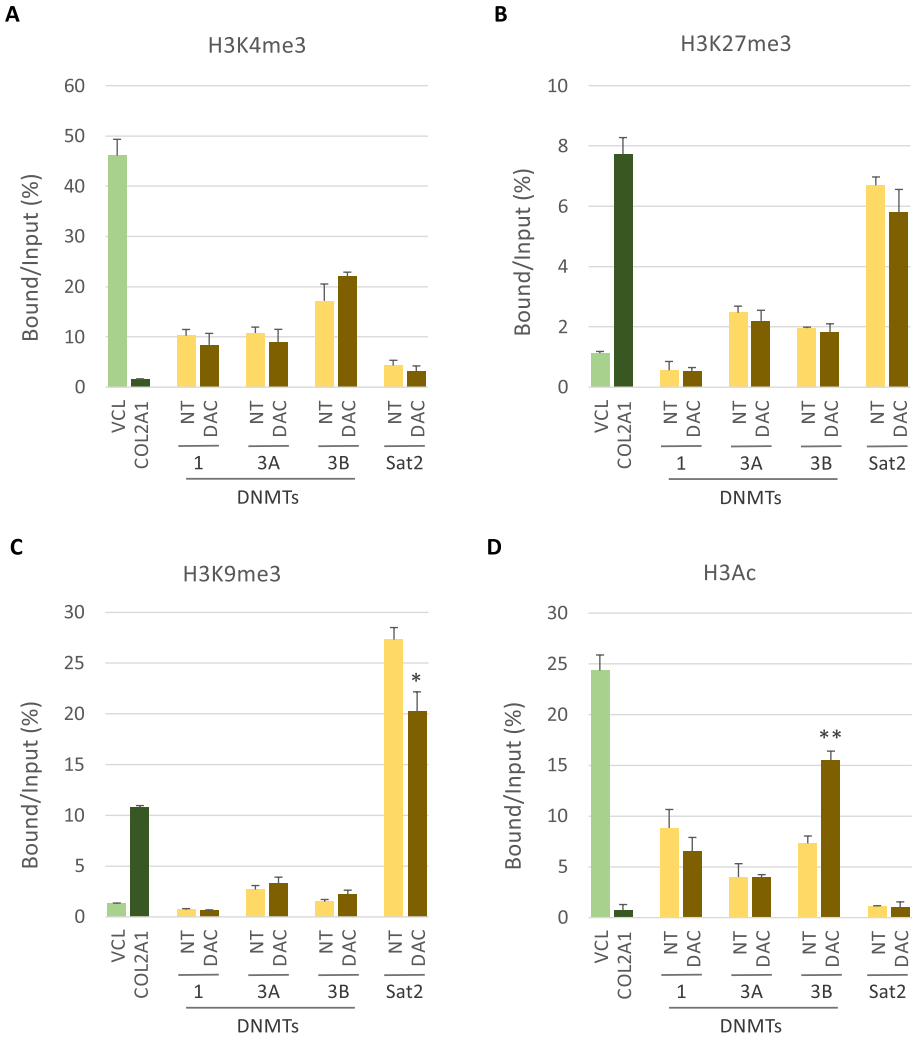

Fig. 5 Effects of DAC on histone post-translational modifications (PTMs) at the DNMTs promoter and satellite 2 repeats. U937 cells were subjected to treatment with decitabine at a concentration of 0.1 μM for 64 h. At the end of treatment, chromatin was extracted and immunoprecipitated with specific antibodies directed against four different histone H3 PTMs. The DNA purified from the bound and input fractions was amplified by real-time qPCR using primer pairs specific for the three DNMT promoters or satellite 2 repeats. The primers used to amplify the active gene vinculin (VCL) and a gene known to be silenced in this cellular model (COL2A1) were used as controls. Data showing the enrichment of each gene promoter as a percentage of bound with respect to the input are shown for H3K4me3 (**A**), H3K27me3 (**B**), H3K9me3 (**C**) and H3 acetylation (**D**). All the experiments were conducted in triplicate. *$P < 0.05$ and **$P < 0.01$ with respect to the untreated (NT) sample

decrease of H3K9me3 was observed in DAC treated cells respect to the untreated cellular population.

These observations are further supported by the similar results obtained using AZA at a concentration of 0.5 μM (Additional Fig. 2).

Discussion

Although azanucleosides are thought to act through the induction of global DNA demethylation and consequent re-expression of aberrantly silenced genes, the induction of other phenomena, such as the DNA damage response due to the covalent trapping of DNMTs on DNA, immunomodulation and the reactivation of endogenous retroelements (EREs), must be considered [5–8]. Several studies have indicated that the demethylation of satellite repeats induced by azanucleosides, and the consequent genomic destabilization and mitotic impairment, could strongly contribute to the effects of these drugs on cancer cells [16–18], especially in MDS and AML, in which, unlike other types of cancer, satellite repeats show normal (high) levels of methylation [15].

The low half-life of DAC and AZA in vivo due to rapid deamination by cytidine deaminase forces the administration of these drugs as short-term (usually 1 h) infusions. Indeed, pharmacokinetic studies have shown that decitabine is rapidly eliminated from human plasma and is no longer detectable approximately 30–40 min after the end of the infusion [31, 32].

The demethylating effect of DAC at CpG islands has already been investigated in AML cell lines and patients through genome-wide studies suggesting a non-random demethylating activity. Yan and colleagues, for example, demonstrate that decitabine induces significant methylation changes in posttreatment patient's bone marrows. Specifically, their data showed that DNA hypomethylation occurred mainly in promoter CpG islands respect to CpG related to other genomic features [39]. Negrotto and colleagues showed that CpGs that are usually hypomethylated during granulocyte maturation were significantly hypermethylated in AML cells and that decitabine-induced hypomethylation was greatest at these CpGs and was accompanied by cellular differentiation of AML cells [40]. More recently, Greve and colleagues evaluated the effects of DAC treatments in patients comparing the genome-wide effects on methylation between AML blasts and T-cells, observing a massive, non-random demethylation in AML blasts and, in contrast, a thousand-fold lesser, random demethylation, in T-cells, indicating selectivity of the demethylation for the malignant blasts [41].

In addition, other studies explored the stability of HMA-induced demethylation, demonstrating a regain of methylation only after several days of culture in drug-free medium, suggesting long-term stability of demethylation at promoter CpG islands [42–44]. However, little is known about the effects of HMA on pericentromeric satellite sequences, also due to the well-known challenge of uniquely mapping reads in repetitive regions, which limits the analysis of such sequences in NGS studies.

This study aims to investigate in vitro the dynamics of the effects of azanucleosides on the methylation levels of satellite 2 repeats [25–30]. The acute myeloid leukemia (AML) U937 cell line, which is known to have normal (high) satellite 2 methylation levels [45], was used in this study as a model.

Although the effects of HMAs on DNMT1 inhibition have been widely documented in the literature, the effects on DNMT3A and DNMT3B are much more controversial [46]. We found that the strong initial demethylation of satellite 2 repeats after 16 h of treatment with both DAC and AZA, followed by a complete regain of methylation after only 48 h of culture, in agreement with the previous observation that bone marrow mononuclear cells from MDS patients, which show satellite 2 demethylation during DAC treatment, achieve complete remethylation when the treatment course ends [47]. This finding drove us to monitor the effects of the treatments on the expression of the enzymes involved in DNA methylation, revealing significant upregulation of both the active (DNMT3B1/2) and inactive regulatory (DNMT3B3) DNMT3B isoforms. Despite being catalytically inactive, DNMT3B3 is known to positively regulate the de novo methylation activity of the active DNMT3B isoforms [33], and its upregulation is indicative of further strengthening of DNMT3B activity. This finding is not surprising if we consider the known role of DNMT3B in satellite 2 methylation [48, 49]. However, although the concomitant remethylation of satellite 2 repeats at 64 h of treatment and the upregulation of DNMT3B observed in this study suggest a role for this regulation in the regain of methylation observed at satellite repeats, at this stage of knowledge this relation can be only hypothesized.

The known ability of AZA and DAC to demethylate and reactivate the expression of silenced genes led us to hypothesize that the observed upregulation of the DNMT3B transcript could be related to the demethylation of its promoter. However, the analysis of the DNMT3B promoter methylation status via MS-HRM revealed a low basal level of methylation, with a slight DAC-dependent decrease in methylation at the higher concentrations tested, suggesting that the demethylation of the DNMT3B promoter is not the basis of the observed DNMT3B upregulation. However, since some studies reported that the methylation status of a single CpG can influence the transcription of related genes [50–53], the role of this phenomenon cannot be completely excluded but should be demonstrated.

The weak effect on DNMT3B promoter methylation prompted us to investigate the status of its histone PTMs via chromatin immunoprecipitation (ChIP). Histone H3 trimethylations at lysines 4, 9 and 27 were investigated together with histone H3 acetylation. H3K4me3 is known to be associated with active transcription, whereas H3K9me3 and H3K27me3 are associated with silencing [54]. In particular, H3K9 methylation and DNA methylation are strongly associated and work synergistically to form heterochromatin to silence genes and retrotransposons [35]. However, we found that azanucleosides did not affect the level of histone H3 methylation. In contrast, we observed a significant increase in histone H3 acetylation levels at the DNMT3B promoter with both DAC and AZA, whereas no changes in histone H3 acetylation were detected at the other DNMT promoters. These data are in line with gene expression studies in which the DNMT3B transcript was the only DNMT that was regulated, suggesting a role of histone H3 acetylation in the monitored DNMT3B upregulation.

However, at this stage, the mechanism underlying the increase in histone H3 acetylation at the DNMT3B promoter can only be hypothesized. DNA methylation and histone acetylation are coupled by SIN3 and NuRD complexes, which harbor histone deacetylase (HDAC) activity and are recruited by methyl-binding proteins such as MeCP2 and MBD2 to methylated DNA [55–57]. However, even in this case, the weak change in DNA methylation at the DNMT3B promoter does not seem to explain

the increase in acetylation and the consequent transcriptional upregulation.

In contrast, it is reasonable to speculate that the increased histone H3 acetylation and expression of DNMT3B could be the result of the cell response to the demethylation of its satellite repeats with the goal of restoring normal levels of methylation, allowing correct cellular replication and, thus, survival. In this context, it is possible that DNMT3B upregulation could limit the activity of HMAs, counteracting the genomic destabilization and impairment of mitosis resulting from satellite DNA demethylation. DNMT3B is indeed frequently upregulated in cancer, and its expression has been associated with poor prognosis in AML and other malignancies [58–62].

The effects of HMAs on PTMs at satellite 2 repeats were also examined, revealing no significant changes, except for a decrease in H3K9me3 levels after 64 h of DAC treatment. This finding is consistent with the satellite 2 methylation pattern observed by Southern blotting, which shows a strong but incomplete recovery of the demethylated state detected after 16 h of treatment. This observation is in line with the well-known interplay between DNA methylation and H3K9me3 in the establishment and maintenance of heterochromatin at satellite repeats [63].

The study herein presented is preliminary and has limitations. First, all the experiments herein presented has been conducted using a single AML cell line and should be extended in the future to other AML or even not-AML cell lines to generalize the observations reported in this work. Secondly, the relation between satellite 2 remethylation at 64 h of treatment and the concomitant upregulation of DNMT3B is speculative and can be only suggested even if, as already stated, it must be recognized that the role of DNMT3B in satellite 2 methylation has been widely documented in literature [48, 49].

Conclusions

Satellite DNA repeat demethylation is believed to play an important role in the activity of HMAs. To the best of our knowledge, our study is the first to show that satellite 2 demethylation induced by HMA treatment in the U937 AML cell line is transitory and that remethylation is associated with epigenetic modulation and increased expression of the satellite methyltransferase DNMT3B. However, further studies are necessary to confirm the role of DNMT3B upregulation in satellite 2 regain of methylation, to fully understand the consequences of satellite 2 remethylation and the mechanisms that govern this phenomenon, as well as to evaluate whether the same happens in vivo and, thus, the possible impact of concomitant strategies to limit the satellite 2 remethylation, such as DNMT3B silencing, on the efficacy of azanucleoside treatments in AML and MDS.

Abbreviations

AML	Acute myeloid leukemia
AZA	Vidaza
ChIP	Chromatin immunoprecipitation
COL2A1	Collagen type II alpha 1 chain
DAC	Decitabine
DNMT1	DNA methyltransferase 1
DNMT3A	DNA methyltransferase 3A
DNMT3B	DNA methyltransferase 3B
DNMT	DNA methyltransferase
EREs	Endogenous retroelements
HDAC	Histone deacetylase
HMAs	Hypomethylating agents
HRM	High-resolution melting
HR-MDS	High-risk myelodysplastic syndrome
MDS	Myelodysplastic syndromes
MS-HRM	Methylation-sensitive high-resolution melting
VCL	Vinculin

Supplementary Information

The online version contains supplementary material available at https://doi.org/10.1186/s12885-025-14998-w.

Additional File 1: Additional fig. 1. Effects of vidaza on the methylation status of satellite 2 repeats and the regulation of DNMT expression in U937 cells. U937 cells were subjected to treatments with AZA at the reported concentrations and times or left untreated. (A) Satellite 2 methylation was evaluated by Southern blotting. At the end of the treatments, the genomic DNA was purified and digested using the Csp45I enzyme, separated via 1% agarose gel electrophoresis, blotted, and hybridized using a satellite 2 PCR probe (sat2-384U/781L). Ethidium bromide-stained agarose gel prior of DNA transfer is shown in Additional Figure 4, while full-length blot is reported in Additional Figure 3 (panels C,D). (B) DNMT expression was evaluated by real-time RT–qPCR. Total RNA was purified, reverse transcribed into cDNA and amplified by real-time qPCR using primer pairs specific for the transcripts of different DNMTs (GAPDH was also amplified and used for normalization). Relative quantitation was performed via the 2-ddCt method. All the experiments were conducted in triplicate. *P < 0.05 with respect to the untreated sample (NT); **P < 0.01 with respect to the NT sample. (C) The methylation status of the DNMT3B promoter was investigated by methylation-sensitive high-resolution melting (MS-HRM). U937 cells were subjected to treatments with AZA at the reported concentrations and times or left untreated. At the end of the treatments, genomic DNA was purified, subjected to bisulfite conversion and amplified by PCR using primers specific for the DNMT3B promoter. The resulting PCR products were analyzed by HRM, and the fluorescence signal was normalized via Rotor-Gene Q software. 100%, 0% and 50% are commercial DNA standards representing fully methylated, fully unmethylated and a 1:1 mix of fully methylated and fully unmethylated DNA, respectively. All the experiments were conducted in triplicate.

Additional File 2: Additional fig. 2. Effects of vidaza on histone post-translational modifications (PTMs) at the DNMTs promoter and satellite 2 repeats. U937 cells were subjected to treatment with 0.5 μM AZA for 64 hours. At the end of treatment, chromatin was extracted and immunoprecipitated with specific antibodies directed against four different histone H3 PTMs. The DNA purified from the bound and input fractions was amplified by real-time qPCR using primer pairs specific for the three DNMT promoters or satellite 2 repeats. The primers used to amplify the active gene vinculin (VCL) and a gene known to be silenced in this cellular model (COL2A1) were used as controls. Data showing the enrichment of each gene promoter as a percentage of that bound with respect to the input are shown for H3K4me3 (A), H3K27me3 (B), H3K9me3 (C) and H3 acetylation (D). All the experiments were conducted in triplicate. *P < 0.05 and **P < 0.01 with respect to the untreated (NT) sample.

Additional File 3: Additional fig. 3. Agarose gel used in the Southern blot

experiment reported in Figure 2. U937 cells were subjected to treatments with DAC at the reported concentrations and times or left untreated (NT). At the end of the treatments, genomic DNA was purified and digested via the Csp45I enzyme, separated via 1% agarose gel electrophoresis, and stained with ethidium bromide. Other samples: samples from another project not related to the work presented in this manuscript. MK II: commercial DNA molecular ladder from Roche. NIH-3T3: genomic extracted from murine cells used as control of probe hybridization. Not dig. probe: not-digoxigenated probe used as positive control of probe hybridization. The dotted line rectangle indicates the area of the gel reported in the manuscript blots figures.

Additional File 4: Additional fig. 4. Agarose gel used in the Southern blot experiment reported in Additional Figure 1. U937 cells were subjected to treatments with AZA at the reported concentrations and times or left untreated (NT). At the end of the treatments, genomic DNA was purified and digested via the Csp45I enzyme, separated via 1% agarose gel electrophoresis, and stained with ethidium bromide. MK II: commercial DNA molecular ladder from Roche. Solid tumors-derived cell lines T98G and U-373MG were used as control of mild and heavy satellite 2 demethylation, respectively [20]. Not dig. probe: not-digoxigenated probe used as positive control of probe hybridization. Dotted line rectangles indicate the areas of the blot reported in the manuscript figures.

Additional File 5: Additional fig. 5. Uncropped blots. Uncropped blots used for Figure 2 and Additional Figure 1 (panel A) are shown at different exposure levels. (A,B) U937 cells were subjected to treatments with DAC at the reported concentrations and times or left untreated (NT). At the end of the treatments, genomic DNA was purified and digested via the Csp45I enzyme, separated via 1% agarose gel electrophoresis, blotted, and hybridized by a satellite 2 PCR probe (sat2-384U/781L). Other samples: samples from another project not related to the work presented in this manuscript. Not dig. probe: not-digoxigenated probe used as positive control of probe hybridization. Spotted dig. probe: digoxigenated probe spotted in the filter used as positive control of anti-digoxigenin antibody binding. Dotted line rectangles indicate the areas of the blot reported in the manuscript figures. Arrows in panel B indicate the corners of the membrane. (C,D) U937 cells were subjected to treatments with AZA at the reported concentrations and times or left untreated (NT). At the end of the treatments, genomic DNA was purified and digested via the Csp45I enzyme, separated via 1% agarose gel electrophoresis, blotted, and hybridized by a satellite 2 PCR probe (sat2-384U/781L). Solid tumors-derived cell lines T98G and U-373MG were used as control of mild and heavy satellite 2 demethylation, respectively [20]. Samples treated with 1 μM AZA were not considered in the study in consequence of the high level of cytotoxicity monitored at this condition of treatment. Not dig. probe: not-digoxigenated probe used as positive control of probe hybridization. Spotted dig. probe: digoxigenated probe spotted in the filter used as positive control of anti-digoxigenin antibody binding. Dotted line rectangles indicate the areas of the blot reported in the manuscript figures. Arrows in panel D indicate the corners of the membrane.

Acknowledgements
We would like to express our gratitude to Dr. Giulia Peverini for the editing and English revision of the manuscript.

Authors' contributions
Enrica Sordini: Investigation, Data Curation. Eugenia Ciurlia: Investigation, Data curation. Alessia Zanella: Investigation, Data curation. Benedetta Fogliardi: Investigation, Data curation. Dorela Lame: Investigation, Data curation. Antonella Poloni: Supervision, Review and Editing. Stefano Amatori: Conceptualization, supervision, writing—original draft, reviewing and editing. Mirco Fanelli: Conceptualization, supervision, writing, reviewing and editing.

Funding
This work was supported by Fanoateno.

Data availability
The datasets used and/or analyzed during the current study are available from the corresponding author on reasonable request.

Declarations

Ethics approval and consent to participate
Not applicable.

Consent for publication
Not applicable.

Competing interests
The authors declare no competing interests.

Author details
[1]Molecular Pathology Laboratory "PaoLa", Department of Biomolecular Sciences, University of Urbino Carlo Bo, Fano, PU, Italy
[2]Department of Clinical and Molecular Sciences, Hematology Unit, Università Politecnica Delle Marche, Ancona, Italy

Received: 26 June 2025 / Accepted: 4 September 2025
Published online: 18 November 2025

References

1. Platzbecker U, Kubasch AS, Homer-Bouthiette C, Prebet T. Current challenges and unmet medical needs in myelodysplastic syndromes. Leukemia. 2021;35:2182–98.
2. Kantarjian HM, et al. Acute myeloid leukemia: historical perspective and progress in research and therapy over 5 decades. Clin Lymphoma Myeloma Leuk. 2021;21:580–97.
3. Hemmati S, Haque T, Gritsman K. Inflammatory signaling pathways in preleukemic and leukemic stem cells. Front Oncol. 2017;7:265.
4. Ogawa S. Genetics of MDS. Blood. 2019;133:1049–59.
5. Agrawal K, Das V, Vyas P, Hajduch M. Nucleosidic DNA demethylating epigenetic drugs-a comprehensive review from discovery to clinic. Pharmacol Ther. 2018;188:45–79.
6. Sigalotti L, et al. Epigenetic drugs as pleiotropic agents in cancer treatment: biomolecular aspects and clinical applications. J Cell Physiol. 2007;212:330–44.
7. Stresemann C, Lyko F. Modes of action of the DNA methyltransferase inhibitors azacytidine and decitabine. Int J Cancer. 2018;123:8–13.
8. Kordella C, Lamprianidou E, Kotsianidis I. Mechanisms of action of hypomethylating agents: endogenous retroelements at the epicenter. Front Oncol. 2021;11:650473.
9. Zeidan AM, et al. Counseling patients with higher-risk MDS regarding survival with azacitidine therapy: are we using realistic estimates? Blood Cancer J. 2018;8:55.
10. Dombret H, et al. International phase 3 study of azacitidine vs conventional care regimens in older patients with newly diagnosed AML with >30% blasts. Blood. 2015;126:291–9.
11. Mattei AL, Bailly N, Meissner A. DNA methylation: a historical perspective. Trends Genet. 2022;38:676–707.
12. Hagemann S, Heil O, Lyko F, Brueckner B. Azacytidine and decitabine induce gene-specific and nonrandom DNA demethylation in human cancer cell lines. PLoS ONE. 2011;7(6):17388.
13. Ehrlich M. DNA methylation in cancer: too much, but also too little. Oncogene. 2002;21:5400–13.
14. Gaudet F, et al. Induction of tumors in mice by genomic hypomethylation. Science. 2003;300:489–99.
15. Maegawa S, et al. Age-related epigenetic drift in the pathogenesis of MDS and AML. Genome Res. 2014;24:580–91.
16. Hernandez R, Frady A, Zhang XY, Varela M, Ehrlich M. Preferential induction of chromosome 1 multibranched figures and whole-arm deletions in a human pro-B cell line treated with 5-azacytidine or 5-azadeoxycytidine. Cytogenet Cell Genet. 1997;76:196–201.
17. Costa G, Barra V, Lentini L, Cilluffo D, Di Leonardo A. DNA demethylation caused by 5-Aza-2'-deoxycytidine induces mitotic alterations and aneuploidy. Oncotarget. 2016;7:3726–39.
18. Prada D, et al. Satellite 2 demethylation induced by 5-azacytidine is associated with missegregation of chromosomes 1 and 16 in human somatic cells. Mutat Res. 2012;729:100–5.
19. Greenberg PL, et al. NCCN guidelines® insights: myelodysplastic syndromes, version 3.2022. J Natl Compr Canc Netw. 2022;20:106–17.

20. Fanelli M, et al. Loss of pericentromeric DNA methylation pattern in human glioblastoma is associated with altered DNA methyltransferases expression and involves the stem cell compartment. Oncogene. 2008;27:358–65.
21. Hassan KM, Norwood T, Gimelli G, Gartler SM, Hansen RS. Satellite 2 methylation patterns in normal and ICF syndrome cells and association of hypomethylation with advanced replication. Hum Genet. 2001;109:452–62.
22. Faversani A, et al. MiR-494-3p is a novel tumor driver of lung carcinogenesis. Oncotarget. 2017;8:7231–47.
23. Guerzoni C, et al. An aza-macrocycle containing maltolic side-arms (maltonis) as potential drug against human pediatric sarcomas. BMC Cancer. 2014;14:137.
24. Flebbe H, et al. Epigenome mapping identifies tumor-specific gene expression in primary rectal cancer. Cancers (Basel). 2019;11(8):1142.
25. Bouck N, Kokkinakis D, Ostrowsky J. Induction of a step in carcinogenesis that is normally associated with mutagenesis by nonmutagenic concentrations of 5-azacytidine. Mol Cell Biol. 1984;4:1231–7.
26. Haaf T. The effects of 5-azacytidine and 5-azadeoxycytidine on chromosome structure and function: implications for methylation-associated cellular processes. Pharmacol Ther. 1995;65:19–46.
27. Rudek MA, Zhao M, He P, Hartke C, Gilbert J, Gore SD, et al. Pharmacokinetics of 5-azacitidine administered with phenylbutyrate in patients with refractory solid tumors or hematologic malignancies. J Clin Oncol. 2005;23:3906–11.
28. Liu Z, et al. Characterization of decomposition products and preclinical and low dose clinical pharmacokinetics of decitabine (5-aza-2′-deoxycytidine) by a new liquid chromatography/tandem mass spectrometry quantification method. Rapid Commun Mass Spectrom. 2006;20:1117–26.
29. Yoo CB, et al. Delivery of 5-aza-2′-deoxycytidine to cells using oligodeoxynucleotides. Cancer Res. 2007;67:6400–8.
30. Stresemann C, Lyko F. Modes of action of the DNA methyltransferase inhibitors azacytidine and decitabine. Int J Cancer. 2008;123:8–13.
31. Karahoca M, Momparler RL. Pharmacokinetic and pharmacodynamic analysis of 5-aza-2′-deoxycytidine (decitabine) in the design of its dose-schedule for cancer therapy. Clin Epigenetics. 2013;5:3.
32. Cashen AF, Shah AK, Todt L, Fisher N, DiPersio J. Pharmacokinetics of decitabine administered as a 3-h infusion to patients with acute myeloid leukemia (AML) or myelodysplastic syndrome (MDS). Cancer Chemother Pharmacol. 2008;61:759–66.
33. Zeng Y, et al. The inactive Dnmt3b3 isoform preferentially enhances Dnmt3b-mediated DNA methylation. Genes Dev. 2020;34:1546–58.
34. Gujar H, Weisenberger DJ, Liang G. The roles of human DNA methyltransferases and their isoforms in shaping the epigenome. Genes. 2019;10:172.
35. Janssen SM, Lorincz MC. Interplay between chromatin marks in development and disease. Nat Rev Genet. 2022;23:137–53.
36. Nan X, et al. Transcriptional repression by the methyl-CpG-binding protein MeCP2 involves a histone deacetylase complex. Nature. 1998;393:386–9.
37. Zhang Y, et al. Analysis of the NuRD subunits reveals a histone deacetylase core complex and a connection with DNA methylation. Genes Dev. 1999;13:1924–35.
38. Yoon HG, Chan DW, Reynolds AB, Qin J, Wong J. N-coR mediates DNA methylation-dependent repression through a methyl CpG binding protein Kaiso. Mol Cell. 2003;12:723–34.
39. Yan P, et al. Genome-wide methylation profiling in decitabine-treated patients with acute myeloid leukemia. Blood. 2012;120(12):2466–74.
40. Negrotto S, et al. CpG methylation patterns and decitabine treatment response in acute myeloid leukemia cells and normal hematopoietic precursors. Leukemia. 2012;26(2):244–54.
41. Greve G, et al. In vivo kinetics of early, non-random methylome and transcriptome changes induced by DNA-hypomethylating treatment in primary AML blasts. Leukemia. 2023;37:1018–27.
42. Yang X, et al. Gene body methylation can alter gene expression and is a therapeutic target in cancer. Cancer Cell. 2014;26:577–90.
43. Kagey JD, Kapoor-Vazirani P, McCabe MT, Powell DR, Vertino PM. Long-term stability of demethylation after transient exposure to 5-aza-2′-deoxycytidine correlates with sustained RNA polymerase II occupancy. Mol Cancer Res. 2010;8:1048–59.
44. Tsai HC, et al. Transient low doses of DNA-demethylating agents exert durable antitumor effects on hematological and epithelial tumor cells. Cancer Cell. 2012;21:430–46.
45. Amatori S, et al. Decitabine, differently from DNMT1 silencing, exerts its antiproliferative activity through p21 upregulation in malignant pleural mesothelioma (MPM) cells. Lung Cancer. 2009;66:184–90.
46. Wong KK, Lawrie CH, Green TM. Oncogenic roles and inhibitors of DNMT1, DNMT3A, and DNMT3B in acute myeloid leukaemia. Biomark Insights. 2019;14:1177271919846454.
47. Mund C, Hackanson B, Stresemann C, Lübbert M, Lyko F. Characterization of DNA demethylation effects induced by 5-Aza-2′-deoxycytidine in patients with myelodysplastic syndrome. Cancer Res. 2005;65:7086–90.
48. Xu GL, et al. Chromosome instability and immunodeficiency syndrome caused by mutations in a DNA methyltransferase gene. Nature. 1999;402:187–91.
49. Hansen RS, et al. The DNMT3B DNA methyltransferase gene is mutated in the ICF immunodeficiency syndrome. Proc Natl Acad Sci U S A. 1999;96:14412–7.
50. Robertson KD, Hayward SD, Ling PD, Samid D, Ambinder RF. Transcriptional activation of the Epstein-Barr virus latency C promoter after 5-azacytidine treatment: evidence that demethylation at a single CpG site is crucial. Mol Cell Biol. 1995;15:6150–9.
51. Claus R, et al. Quantitative DNA methylation analysis identifies a single CpG dinucleotide important for ZAP-70 expression and predictive of prognosis in chronic lymphocytic leukemia. J Clin Oncol. 2012;30:2483–91.
52. Sobiak B, Leśniak W. The effect of single CpG demethylation on the pattern of DNA-protein binding. Int J Mol Sci. 2019;20:914.
53. Ceccarelli V, et al. Eicosapentaenoic acid demethylates a single CpG that mediates expression of tumor suppressor CCAAT/enhancer-binding protein delta in U937 leukemia cells. J Biol Chem. 2011;286:27092–102.
54. Shirvaliloo M. The landscape of histone modifications in epigenomics since 2020. Epigenomics. 2022;14:1465–77.
55. Nakao M. Epigenetics: interaction of DNA methylation and chromatin. Gene. 2001;278:25–31.
56. Reid XJ, Low JKK, Mackay JP. A NuRD for all seasons. Trends Biochem Sci. 2023;48:11–25.
57. Della Ragione F, Vacca M, Fioriniello S, Pepe G, D'Esposito M. MECP2, a multitalented modulator of chromatin architecture. Brief Funct Genomics. 2016;15:420–31.
58. Niederwieser C, et al. Prognostic and biologic significance of DNMT3B expression in older patients with cytogenetically normal primary acute myeloid leukemia. Leukemia. 2015;29:567–75.
59. Chen WC, Chen MF, Lin PY. Significance of DNMT3b in oral cancer. PLoS ONE. 2014;9:e89956.
60. Hayette S, et al. High DNA methyltransferase DNMT3B levels: a poor prognostic marker in acute myeloid leukemia. PLoS ONE. 2012;7:e51527.
61. Lamba JK, et al. Integrated epigenetic and genetic analysis identifies markers of prognostic significance in pediatric acute myeloid leukemia. Oncotarget. 2018;9:26711–23.
62. Gagliardi M, Strazzullo M, Matarazzo MR. DNMT3B functions: novel insights from human disease. Front Cell Dev Biol. 2018;6:140.
63. Nicetto D, Kenneth SZ. Role of H3K9me3 heterochromatin in cell identity establishment and maintenance. Curr Opin Genet Dev. 2019;55:1–10.

Publisher's Note